GREM2 is associated with human central obesity and inhibits visceral preadipocyte browning

Wen Liu,[a,b,1] Danjie Li,[a,1] Minglan Yang,[a,1] Long Wang,[a,1] Yu Xu,[a,1] Na Chen,[a] Zhiyin Zhang,[a] Juan Shi,[a] Wen Li,[a] Shaoqian Zhao,[a] Aibo Gao,[a] Yufei Chen,[a] Qinyun Ma,[a] Ruizhi Zheng,[a] Shujing Wu,[a] Yifei Zhang,[a] Yuhong Chen,[a] Shuwen Qian,[c] Yufang Bi,[a] Weiqiong Gu,[a] Qiqun Tang,[c] Guang Ning,[a,b] Ruixin Liu,[a] Weiqing Wang,[a] Jie Hong,[a] and Jiqiu Wang [a,b]*

[a]Department of Endocrine and Metabolic Diseases, Shanghai Institute of Endocrine and Metabolic Diseases, Ruijin Hospital, Shanghai Jiao Tong University School of Medicine, Shanghai, China
[b]Shanghai National Clinical Research Center for Metabolic Diseases, Key Laboratory for Endocrine and Metabolic Diseases of the National Health Commission of the PR China, Shanghai Key Laboratory for Endoceine Tumor, State Key Laboratory of Medical Genomics, Ruijin Hospital, Shanghai Jiao Tong University School of Medicine, Shanghai, China
[c]The Key Laboratory of Metabolism and Molecular Medicine of the Ministry of Education, Department of Biochemistry and Molecular Biology of School of Basic Medical Sciences, Fudan University Shanghai Medical College, Shanghai, China

Summary

Background Some circulating proteins are linked to central adiposity. Gremlin 2 (GREM2) functions as a secreted factor involved in osteogenesis and adipogenesis. Here, we investigated the association of blood GREM2 levels and central adiposity, and the biological roles of GREM2 in the browning program of visceral preadipocytes.

Methods Three independent cohorts were applied to detect circulating GREM2 levels. Recombinant Grem2 protein, *Grem2* overexpression and knockout mouse models, and preadipocyte-specific *Bmpr2* knockout mice were used to assess the roles of Grem2 in the browning program.

Findings We detected the presence of GREM2 protein in human serum using an ELISA approach. We revealed elevated GREM2 levels in severely obese subjects and validated this finding in a large-scale community population involving 10,327 subjects. Notably, serum GREM2 was positively associated with visceral fat volume, as quantified by 3D reconstruction methods. In mice, Grem2 was highly expressed in visceral fat and liver tissues, while surgical removal of visceral fat lowered circulating Grem2 levels. Visceral fat secreted more Grem2 in obese mice. *Grem2*-overexpressed mice exhibited a reduced browning ability of visceral fat, whereas *Grem2* ablation enhanced the browning capacity and reduced visceral fat content. Mechanistically, Grem2 attenuated the browning program of visceral preadipocytes partially by antagonizing BMP4/7-SMAD1/5/8 signaling pathway. Further, genetic deletion of *Bmpr2* in Pdgfrα+ preadipocytes abolished the antagonistic effect of Grem2.

Interpretation These findings indicate that GREM2 might function as a circulating protein factor associated with human visceral adiposity, and Grem2 inhibits the browning capacity of visceral preadipocytes partially by BMP4/7-BMPR2 signaling pathway.

Funding The complete list of funders can be found in the Acknowledgement section.

Keywords: GREM2; Serum biomarker; Central obesity; Visceral fat; Browning

Introduction

Obesity has become a growing epidemic worldwide in recent decades and is associated with a series of leading causes of death.[1,2] Unlike general obesity, central obesity is characterized by excessive visceral fat accumulation, which is particularly vulnerable to lipid overload and is recognized as a driver of cardiometabolic diseases.[3,4] One challenge in combating central obesity is that there are few effective and safe strategies to lose visceral fat once it has been deposited.[3] Although the reasons for depot-specific fat deposition remain unclear, visceral fat accumulation is partially attributed to the reduced mitochondrial respiratory function and oxidative phosphorylation of visceral adipocytes when compared with subcutaneous adipocytes.[5]

---

*Corresponding author.
E-mail address: wangjq@shsmu.edu.cn (J. Wang).
[1] These authors contribute equally to this work.

Research in context

Evidence before this study

GREM2 is a secreted protein and functions to antagonize the biological roles of BMP2/4 in regulating osteogenesis of stromal cells and adipogenesis of preadipocytes. Visceral fat has a weak browning capacity to some extent attributed to impairment of BMPs-SMADs signaling. Excess visceral fat deposit is tightly associated with malignant metabolic consequences, e.g., type 2 diabetes and cardiovascular diseases. Therefore, this study aims to investigate whether circulating GREM2 levels is associated with human visceral adiposity, and how GREM2 regulates the browning program of visceral preadipocytes.

Added value of this study

This study reports that circulating GREM2 levels are positively associated with visceral obesity in humans, and are especially higher in normal-weight subjects with central obesity. In mice, Grem2 is highly expressed in visceral fat and its expression changes in response to external cues like coldness and fasting-refeeding. Visceral fat of *ob/ob* mice secreted more Grem2. Overexpression of Grem2 attenuates while ablation of Grem2 enhances the browning abilities of visceral fat. Moreover, Grem2 inhibits the browning adipocyte differentiation partially by antagonizing BMP4/7-BMPR2-SMADs signaling in preadipocytes.

Implications of all the available evidence

Circulating GREM2 may be applied as a circulating biomarker for visceral adiposity. The findings highlight the possibility of targeting GREM2 and its downstream pathways for clinical intervention of human visceral adiposity.

Brown adipocytes have a high mitochondria content and powerful capacity to metabolize fatty acids into heat.[6] Emerging evidence has shown that brown-like (beige) adipocytes can originate from progenitors or preadipocytes in stromal vascular fractions (SVFs) of subcutaneous white adipose tissue (sWAT), which functionally and morphologically resembles classical brown adipocytes and has the potential to treat obesity.[7] In contrast, visceral white adipose tissue (vWAT) located deeper in the abdominal cavity shows resistance to browning inducers.[8] Visfatin, which is highly secreted from visceral fat both in humans and mice, was once reported to be correlated with visceral adiposity and exerted insulin-mimetic effects,[9] but these findings has not been well validated by subsequent studies.[10] Theoretically, identifying unknown adipokines associated vWAT may provide a potential way to stratify obesity or even reduce central adiposity.[3]

Among the secreted factors from adipose tissues, decreased activities of the transforming growth factor-β (TGF-β)/bone morphogenetic protein (BMP) signaling pathways are considered to involve in fat accumulation and obesity development.[11–13] As two attractive BMPs, BMP4 mediates the browning of white adipose tissues (WATs) to improve glucose and energy homeostasis,[12] while BMP7 acts as a key regulator of classical brown adipose tissue (BAT) development.[14] In comparison with BMP members, few studies have investigated the clinical implications and biological roles of BMP antagonists in metabolic disorders, among which Gremlin 2 (GREM2) was reported to increase in adipose tissues with aging[15] and regulate the adipogenesis[16] and osteogenesis.[17] However, the effects of GREM2 on the browning program and central obesity are poorly understood.

GREM2, which was previously named PRDC (Protein Related to DAN and Cerberus) and is recognized as a secreted protein, belongs to the differential screening-selected gene aberrative in the neuroblastoma (DAN) family and can bind to certain BMPs with high affinity, acting as an extracellular BMP antagonist.[18] In our previous study, the GREM2 signal was initially screened out from the expression profile of visceral WAT in *Lgr4*-deficient mice (GSE195570), which exhibited marked visceral browning and obesity-resistant phenotypes.[19] We hypothesized that GREM2 might be involved in the browning process and obesity development. We first found that GREM2 can be detected in the circulating system, and its levels were associated with central obesity in three independent Chinese cohorts. Furthermore, we investigated the biological roles and potential mechanism of GREM2 in the browning process of visceral (pre)adipocytes both *in vitro* and *in vivo*. This study may provide us a circulating biomarker for visceral adiposity and a potential target for clinical intervention of central obesity.

Methods

Human participants

In this study, three independent cohorts were included to evaluate the association between circulating GREM2 levels and adiposity. In the discovery stage, the Genetics of Obesity in Chinese Youngs (GOCY) study that recruited young, severely obese patients was applied. The detailed information of this cohort was described previously and registered in ClinicalTrials.gov (Clinical trial reg. no. NCT01084967, https://clinicaltrials.gov).[19–21] In the validation stage, we utilized a general population including 10,327 participants from a community-based health survey in Jiading District, Shanghai.[22,23] The third cohort was from a deep phenotyping study, which was designed as a longitudinal follow-up of metabolic diseases at SAIC Volkswagen Automotive Company Limited, Shanghai (MedSV

study).[24,25] In the third cohort, we further performed visceral fat mass estimation using three-dimensional (3D) computed tomography (CT) reconstruction in 576 volunteers.[24] Cross-sectional subcutaneous and visceral fat areas were measured at the umbilical level and calculated using FatScan software (N2 Systems Inc).[20,26] The volume of subcutaneous and visceral fat was calculated as volume = number of voxels × voxel size, where voxel size was obtained from Digital Imaging and Communications in Medicine (DICOM) information from corresponding CT images. In all cohorts, anthropometric examinations were performed according to standard protocols, and circulating GREM2 levels were determined using a commercial Grem2 ELISA kit (dy2069, R&D) according to the manufacturer's protocol.

Mice

In the epididymal white adipose tissue (eWAT)-surgical removal experiment, eight male C57BL/6 mice had their epididymal fat pads on both sides excised completely. Eight sham-treated mice underwent the same surgical procedure without fat pad excision. The mice were euthanized for blood collection 10 days after surgery. In the cold stress experiments, mice were subjected to cold room stress (6 °C) for 24 h or 10 days before sample collection. Global $Grem2$ transgenic and $Grem2^{floxp/floxp}$ mice were first generated by a commercial provider (Cyagen) (see supplementary figures). Global $Grem2$ transgenic, $Grem2^{floxp/floxp};aP2$-cre mice and their littermates were subjected to cold room stress (6 °C) for 10 days before euthanasia. Tissue samples were collected from animals after euthanasia and stored in −80 °C freezer or in 4% paraformaldehyde (PFA) until use. Preadipocyte $Bmpr2$ knockout mice were generated by crossing $Bmpr2^{floxp/floxp}$ mice[27] with $Pdgfr\alpha$-cre (JAX stock No. 013148) mice. Homozygous $floxp$ with cre-negative mice was used as controls. The mice were maintained on a 12h:12h light-dark cycle with free access to water and normal chow diet (NCD). A metabolic cage (Columbus Instruments) was used to evaluate the energy expenditure and food intake.[19] ob/ob (B6/JGpt-$Lep^{em1Cd25}$/Gpt, stock no. T001461, RRID: IMSR_GPT:T001461) and wild-type (WT) (n = 7:7) littermate mice were obtained from GemPharmatech. Sample sizes were estimated from previous experience and routine protocols of animal studies, and no additional statistical method was used to predetermine sample size. No randomization was performed during the experiment. Investigators were not blinded when carrying out the experiment, but were blinded during the allocation and sample collection. Inclusion/exclusion criteria is pre-established before the experiments. Mice were placed in the same environment and were measured/treated in an alternating order to minimize the confounders that may impact the outcome of the experiments.

Intraperitoneal glucose tolerance test (IPGTT)

Mice were fasted overnight for 16 h and injected with D-glucose (2 g/kg) intraperitoneally for the glucose tolerance test. Mouse blood glucose levels were measured with whole blood from the tail vein using a glucose meter (LifeScan).

The purification procedures of recombinant mouse Grem2 protein

Pet21b-mGrem2/BL21 (DE3) was inoculated in LB medium (plus 100 microns/m ampicillin) for 3.5 h. The bacterial cells were collected and centrifuged at 6000 × g for 10 min at 4 °C, followed by resuspension in lysate buffer and ultrasonic crushing. The inclusion bodies were washed by ultrasound treatment and dissolved in the buffer, followed by the application of Superdex 200 (GE Healthcare) molecular sieve chromatography and sulfopropyl (SP) cation exchange chromatography, which was used to collect the mouse Grem2 (mGrem2) components. Next, mGrem2 obtained by SP cation exchange chromatography was renatured and refined by Mono S cation exchange chromatography and Superdex 75 (GE Healthcare) molecular sieve to remove polymers and obtain pure mGREM2. The purified mGREM2 was concentrated to 1·6 mg/mL using a 10-KD ultra-filtration concentration tube and stored at −80 °C. Detailed information is provided in Supplementary Figure 1.

Cell culture and plasmid transfection

Human embryonic kidney 293T (HEK293T) cells (ATCC, RRID: CVCL_1926) were cultured in Dulbecco's modified Eagle's medium (DMEM) (Gibco, Cat#10313021) containing 10% fetal bovine serum (FBS) (Gibco, Cat#10270-106) at 37 °C in the presence of 5% CO_2. HEK293T cells were seeded in 24-well plates and transfected with 1·0 μg of pcDNA3.1 vector, vector-expressing plasmid containing the mouse Grem2 (Reference Sequence: NM_011825.1) and human GREM2 (Reference Sequence: NM_022469.4) plasmids, respectively. For co-immunoprecipitation, expression constructs encoding Myc-tagged (C-terminal) human BMP4 or BMP7, and Flag-tagged (C-terminal) mouse Grem2 cDNAs in the pCMV-Entry expression vector were acquired from Xitu company (NM_001202 for BMP4, NM_001719 for BMP7, and NM_011825 for Grem2) and were verified by Sanger sequencing. The plasmids were transfected into HEK293T cells with the Lipofectamine 2000 (Invitrogen, Cat#11668019). Mouse and human recombinant GREM2 proteins used for the evaluation of ELISA kit were purchased from R&D.

Grem2 secretion by visceral fat

In brief, intact unilateral epididymal fat depots were isolated from 8-week-old male *ob/ob* and WT mice, respectively (*n* = 7:7). Every fat pad was then cut into several pieces, placed into a 6-well plate, and covered with a 70 μm strainer to maintain its fully submergence in the culture medium of 6 ml DMEM/F12 (Gibco, Cat#11320082) supplemented with 10% FBS (plus 1% penicillin/streptomycin and 1 mM L-glutamine, Gibco, Cat#15140122, 25030-081). Fat tissues were incubated for 6 h, and the condition media were collected at each time point (1 h, 3 h, and 6 h, respectively).

Stromal vascular fractions (SVFs) isolation and beige adipocyte differentiation

For beige adipocyte induction, the visceral WAT-derived SVFs of humans, male 129S1 mice (Charles River Laboratories), *Grem2*[Tg], *Grem2*[floxp/floxp];*aP2*-cre, or *Bmpr2*[floxp/floxp];*Pdgfrα*-cre mice and their littermate controls were first isolated and then seeded onto 12- or 24-well plates to reach confluence before induction. Beige and white adipocyte induction cocktails were used as previously described.[19] For beige adipocyte induction cocktail, SVFs were initiated to induction with growth medium supplemented with 8·4 μg/ml Insulin, 0·5 mM Isobutylmethylxanthine (IBMX) (Sigma), 1 μM Dexamethasone (DEX) (Sigma), 1 nM Triiodothyronine (T3) (Sigma) and 1 μM Roglitazone (Sigma) for 4 days, and subsequently in growth medium supplemented with 8·4 μg/ml Insulin, 1 nM T3 and 5 μM Roglitazone for the following 4 days. For white adipocyte cocktail, SVFs were induced with growth medium supplemented with 8·4 μg/ml Insulin, 0·5 mM IBMX, 1 μM DEX for 2 days, and in growth medium supplemented with 8·4 μg/ml insulin for the following 6 days. To evaluate the effects of Grem2 on the browning process, recombinant mouse Grem2 protein was added twice (on days -3 and -1, respectively) before the induction procedure. Recombinant human BMP4 or BMP7 proteins (R&D, Cat#MAB757-100, MAB3541-100) were combined with Grem2 in the antagonizing experiments.

Oxygen consumption rate (OCR) measurement

OCRs of differentiated beige adipocytes derived from visceral SVFs were measured at 37 °C using an XF24 analyzer (Seahorse Bioscience) according to the manufacturer's instructions. Oligomycin (1 μM), carbonyl cyanide *p*-(trifluoromethoxy) phenylhydrazone (2 μM), and rotenone/antimycin (1 μM/1 μM) were used to detect basal, uncoupled, maximal, and non-mitochondrial respiration, respectively.

Western blotting assay

Proteins were extracted using the RIPA (Beyotime Biotechnology, Cat#R20095) reagent. All protein concentrations were determined using the BCA protein assay (Thermo fisher, Cat#23227), followed by western blotting as previously described.[19] The resulting bands were visualized using the Imagine Quant LAS 4000 imaging system (GE Healthcare). Detailed information regarding the antibodies is provided in Supplementary Table 1.

Real-time PCR

Total RNA was prepared using the TRIzol reagent (Invitrogen, Cat#15596-018). Real-time PCR was performed with a Quant Studio Real-time PCR Instrument (Applied Biosystems) using SYBR Green Supermix (Takara, Cat#RR420A). Data were normalized to 36B4 expression and analyzed using the $2^{-\Delta\Delta CT}$ method. Detailed primer information is provided in Supplementary Table 2.

Co-immunoprecipitation (co-IP) assay

HEK293T cells were transfected with Myc-tagged BMP4 (or BMP7) and Flag-tagged Grem2 plasmids, and then were collected 24 h later with a NP40 lysis buffer (Beyotime, Cat#P0013F) containing a phosphatase inhibitor cocktail (Roche, Cat#11836153001). After cell lysate was centrifugated at maximum speed, 10% input was taken from the supernatant, and the remaining lysate was incubated with 10 μL Anti-c-Myc magnetic beads (MCE, Cat#HY-K0206) on a rotator overnight at 4 °C. At last, the immunoprecipitate was washed with Np40 for 5 times, and boiled in 2X Laemmli Sample Buffer (Bio-Rad) at 99 °C for 10 min for western blotting analysis.

Staining studies

The staining of Oil Red O (Nanjing Jiancheng Bioengineering Institute) of induced mature beige adipocytes, hematoxylin and eosin (H&E) staining, and immunohistochemical (IHC) staining of uncoupled protein 1 (UCP1) in epididymal fat were performed as previously described,[19] and images were captured using a microscope (Nikon Eclipse Ci-L).

Statistics

In human studies, the distributions of continuous variables were examined by their cumulative frequency distribution charts (proc gchart in SAS). Metabolic indicators, such as body mass index (BMI), waist circumference (WC), waist-height ratio (WHtR), waist-hip ratio (WHR), fasting blood glucose (FBG), HbA1c, total cholesterol, LDL-c, HDL-c, visceral fat area (VFA), visceral fat volume (VFV), and visceral fat content (VFC), presented normal distributions and were presented as the mean ± standard deviation (SD). Other metabolic indicators, such as serum GREM2, triglycerides, fasting insulin, and HOMA-IR, presented non-normally

	Controls	Obesity		P value[1]	P value[2]
	All non-diabetes	**Non-diabetes**	**Diabetes**		
Age (years)	23.39 ± 1.86	23.19 ± 4.35	25.59 ± 6.03	0.9049	0.0410
Sex (men)	146 (52)	147 (57)	17 (8)	0.4664	0.5086
BMI (kg/m^2)	20.18 ± 1.19	36.70 ± 5.29	38.22 ± 4.39	<0.0001	<0.0001
WC (cm)	71.56 ± 5.76	112.48 ± 12.46	115.39 ± 8.28	<0.0001	<0.0001
WHtR	0.43 ± 0.03	0.67 ± 0.07	0.69 ± 0.06	<0.0001	<0.0001
WHR	0.78 ± 0.05	0.95 ± 0.07	0.98 ± 0.05	<0.0001	<0.0001
FBG (mmol/l)	4.78 ± 0.34	5.18 ± 0.54	7.46 ± 1.44	<0.0001	<0.0001
Fasting insulin (IU/ml)	6.16 (4.86−8.09)	21.86 (17.52−30.39)	26.55 (19.50−30.90)	<0.0001	<0.0001
HOMA-IR	1.30 (1.00−1.73)	5.16 (3.82−7.13)	8.09 (7.41−8.85)	<0.0001	<0.0001
HbA1c (%)	5.11 ± 0.24	5.74 ± 0.78	7.31 ± 1.95	<0.0001	<0.0001
Triglycerides (mmol/l)	0.68 (0.56−0.86)	1.51 (1.15−1.91)	1.86 (1.25−2.16)	<0.0001	<0.0001
Total cholesterol (mmol/l)	4.06 ± 0.68	4.53 ± 0.88	5.00 ± 1.21	<0.0001	<0.0001
HDL-c (mmol/l)	1.51 ± 0.29	1.02 ± 0.24	0.97 ± 0.13	<0.0001	<0.0001
LDL-c (mmol/l)	2.17 ± 0.54	2.82 ± 0.74	3.40 ± 0.75	<0.0001	<0.0001
GREM2, pg/ml	924.18 (813.33−1068.65)	1102.71 (988.55−1273.38)	1303.51 (997.42−1467.39)	<0.0001	<0.0001

***Table 1*: The clinical characteristics of young, severely obese subjects and lean controls in GOCY study (*n* = 310).**
Note: Variables with normal distribution data are presented as mean ± SD; Variables with skewed distribution data are presented as median with inter-quartile range. BMI, body mass index; WC, waist circumference; WHtR, waist-height ratio; WHR, waist-hip ratio; FBG, fasting blood glucose; HOMA-IR, homeostasis model assessment for insulin resistance, HOMA-IR = fasting insulin (IU/ml) × fasting glucose (mmol/l)/22.5; HDL-c, high-density lipoprotein cholesterol; LDL-c, low-density lipoprotein cholesterol. P value[1] indicated comparison between obese group and lean control group. P value[2] indicated comparison between non-diabetes and diabetes in obesity group.

distributed and presented as median (interquartile range). To achieve normality, these non-normally distributed values were log-transformed (ln) before analysis. Categorical variables were presented as numbers with proportions. Differences between groups were evaluated by Student's *t*-test (Table 1, Figure 1b) or one-way analysis of variance (ANOVA) (Figure 1a, Supplementary Tables 4 and 6). Pearson correlation analysis was used to explore the correlation between serum lnGREM2 levels and metabolic parameters (Figure 1c,d,h−j and Supplementary Fig. 3). Three logistic regression models were built to investigate the risk of prevalent general obesity and central obesity in relation to each quartile increase in serum GREM2 or each 1-SD increase in lnGREM2. In model 1, no covariates were adjusted. In model 2, age and sex were adjusted. In model 3, age, sex, education level, current alcohol consumption, current smoking habit, physical activity level, diabetes, hypertension, and dyslipidemia status were all adjusted in Jiading study (Table 2 and Supplementary Table 5), while age, sex, diabetes, hypertension, and dyslipidemia status were adjusted in GOCY study as other information was not recorded intactly (Supplementary Table 3). For the *in vivo* and *in vitro* studies, data are expressed as the mean ± standard error (SEM). Two-tailed Student's *t*-test was used for two group comparisons. One-way ANOVA was used for multiple group comparisons. Each experiment was repeated for at least three times. All statistical analyses were performed using SAS software (version 9.4; SAS Institute). Statistical significance was defined as a two-sided *P*-value < 0.05.

Ethics

The human studies were approved by the Institutional Review Board of the Ruijin Hospital, Shanghai Jiao Tong University School of Medicine (SJTUSM) (No. 2010-006) and were in accordance with the principle of the Helsinki Declaration (No. KY2016-75). Written informed consent was obtained from each participant.

Animals used in this study were handled in accordance with the Guide for the Care and Use of Laboratory Animals published by the National Institutes of Health (NIH Publications No. 8023, revised 1978). All animal protocols were reviewed and approved by the Institutional Animal Care and Use Committee (IACUC) of SJTUSM (No. B-2018-005). SJTUSM animal care and use program is accredited by the AAALAC International.

Role of funders

The funders had no role in study design, data collection, data analysis, interpretation, writing of the manuscript, or in the decision to submit the paper for publication.

Results

Human GREM2 measurement with an ELISA method

Human GREM2 (hGREM2) is highly conserved with its homolog, mouse Grem2 (mGrem2), showing 95·2% (160/168 amino acids) identity and 97·6% (164/168 amino acids) similarity (Supplementary Fig. 2a).
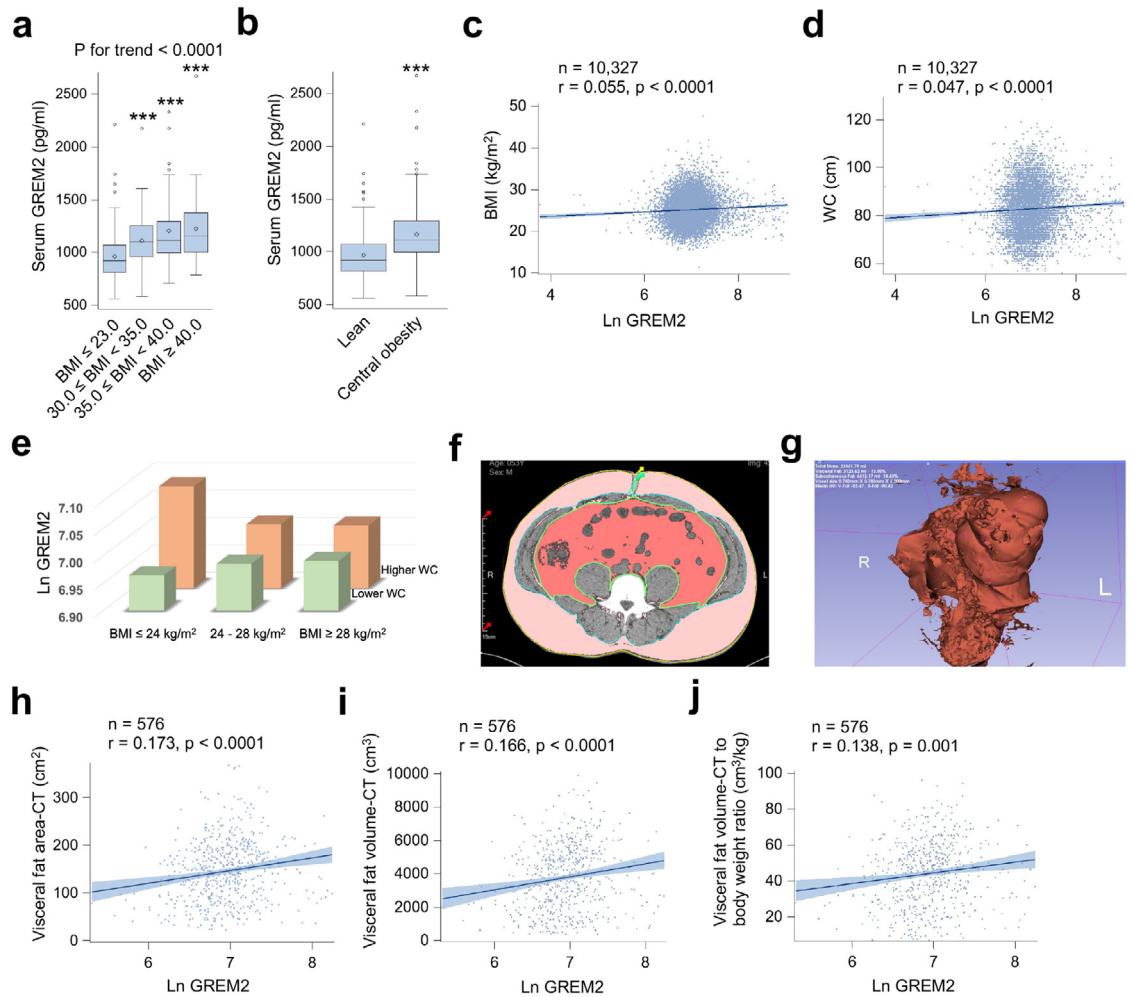
Figure 1. Serum GREM2 levels are elevated in individuals with obesity and positively associated with central obesity. a. The increase trend of serum GREM2 in parallel with the increased BMI in GOCY study (*n* = 146 for lean controls; *n* = 164 for young, severely obese subjects). b. Serum GREM2 levels are higher in GOCY participants with central obesity (*n* = 144 for normal WC; *n* = 160 for central obesity defined by WC; WC data were not recorded intactly for 6 subjects). c-d. The correlation of lnGREM2 and BMI (c) and WC (d), respectively, in the validation population (*n* = 10,327). e. Mean levels of serum GREM2 (lnGREM2) were calculated by the population stratification according to BMI and WC cutoffs. f-g. Visceral fat pads were imaged by CT scanning, and the representative cross-section visceral fat area (VFA) (f) and reconstituted 3D visceral fat volume (VFV) (g) were shown, respectively. h-i. The correlation of serum lnGREM2 levels and VFA (*n* = 576) (h) and VFV (*n* = 576) (i) measurements, respectively. j. The correlation of serum lnGREM2 levels and visceral fat content (VFC) measured (*n* = 576). VFC, visceral fat volume (mL)/body weight (kg). Dose-response association of lnGREM2 with obesity parameters was constructed in linear regression, with shaded area indicating 95% CI. For a, one-way analysis of variance (ANOVA) was used for the multiple group comparisons. For b, two-tailed Student's *t*-test was used for two group comparisons. *** $p < 0.005$.

Therefore, a commercially available mGrem2 ELISA kit was tested to detect hGREM2 protein. After equivalent overexpression of two plasmids in HEK293T cells, mGrem2 and hGREM2 proteins in cell lysates showed comparable expression levels by using an anti-mGrem2 antibody, as well as through measurement by the ELISA kit (Supplementary Fig. 2b,c). Simultaneously, no signals in the vector group were detected, indicating a high specificity of the ELISA detection antibodies. As expected, mGrem2 and hGREM2 were successfully detected in the conditioned media of transfected cells (Supplementary Fig. 2d), indicating that GREM2 is a secreted protein. We also used the ELISA kit to measure commercially available recombinant mGrem2 and hGREM2 proteins and found a high consistency within a wide concentration range, showing a high measurement accuracy (Supplementary Fig. 2e). Two biological supernatant replicates of induced beige adipocytes derived from the SVFs of human visceral fat were used to measure the secreted hGREM2 protein in

	Quartile 1	Quartile 2	Quartile 3	Quartile 4	P for trend
Model 1					
General obesity	1.00	1.23 (0.98−1.54)	1.28 (1.03−1.60)	1.52 (1.23−1.89)	0.0002
Higher WC	1.00	1.31 (1.16−1.48)	1.43 (1.27−1.62)	1.54 (1.37−1.73)	<0.0001
Higher WHtR	1.00	1.27 (1.14−1.42)	1.37 (1.27−1.53)	1.56 (1.39−1.74)	<0.0001
Higher WHR	1.00	1.26 (1.13−1.41)	1.40 (1.25−1.56)	1.49 (1.34−1.67)	<0.0001
Model 2					
General obesity	1.00	1.21 (0.97−1.52)	1.25 (1.00−1.56)	1.47 (1.18−1.82)	0.0008
Higher WC	1.00	1.29 (1.15−1.46)	1.40 (1.24−1.58)	1.48 (1.31−1.67)	<0.0001
Higher WHtR	1.00	1.26 (1.13−1.41)	1.33 (1.19−1.49)	1.47 (1.31−1.65)	<0.0001
Higher WHR	1.00	1.22 (1.09−1.36)	1.32 (1.18−1.47)	1.36 (1.22−1.52)	<0.0001
Model 3					
General obesity	1.00	1.19 (1.02−1.38)	1.25 (1.07−1.45)	1.27 (1.09−1.47)	0.0023
Higher WC	1.00	1.25 (1.11−1.42)	1.29 (1.14−1.46)	1.34 (1.19−1.52)	<0.0001
Higher WHtR	1.00	1.21 (1.08−1.36)	1.22 (1.08−1.37)	1.33 (1.18−1.50)	0.0001
Higher WHR	1.00	1.15 (1.02−1.29)	1.20 (1.07−1.35)	1.20 (1.06−1.35)	0.0021

Table 2: **The risk of general and central obesity in relation to quartiles of serum GREM2 levels in a large-scale population cohort (*n* = 10,327).**
Note:
Model 1 was unadjusted.
Model 2 was adjusted for age and sex.
Model 3 was adjusted for age, sex, education level, current alcohol consumption, current smoking habit, physical activity level, and diabetes, hypertension, and dyslipidemia status.

conditioned media, and they exhibited similar levels and secretion patterns during various differentiation stages (Supplementary Fig. 2f). These results indicate that the mGrem2 ELISA kit could effectively detect hGREM2 protein in extracellular fluids.

Serum GREM2 levels are elevated in the young and severely obese subjects
The GOCY study was initiated to investigate the genetic architecture of the severe obesity in young Chinese.[19,28] In this study, the GOCY cohort recruited 164 young, severely obese subjects (mean BMI ± SD, 36·86 ± 5·22 kg/m²) and 146 lean controls (20·18 ± 1·19 kg/m²). In comparison with lean controls, serum GREM2 levels were higher in subjects with obesity, and the highest in obese patients with diabetes (Table 1). In addition, serum GREM2 levels were positively correlated with metabolic parameters, including FBG, fasting insulin, HOMA-IR, HbA1c, triglycerides, total cholesterol, and LDL-c, but were inversely correlated with HDL-c (Supplementary Fig. 3). We then divided all obese individuals into three subgroups according to their BMI levels. In parallel with the increase in BMI, a significant increasing trend in GREM2 levels was observed after adjusting for age and sex ($P < 0.0001$) (Figure 1a). Waist circumference (WC) is a common clinical parameter used to define central obesity by WC ≥ 90 cm (men) and 85 cm (women), respectively.[29,30] Interestingly, higher serum GREM2 levels were observed in subjects with central obesity

defined by the WC cutoffs after adjusting for age and sex ($P < 0.0001$) (Figure 1b). Next, using binary logistic regression analysis, we found that serum GREM2 levels were positively correlated with general obesity defined by BMI ≥ 30·0 kg/m² (odds ratio [OR]: 1·76, 95% confidential interval [CI]: 1·13−2·75, $P = 0.013$), as well as for central obesity, respectively, defined by the above WC cutoffs (OR: 1·66, 95% CI: 1·07−2·58, $P = 0.023$) or by waist-height ratio (WHtR) ≥ 0·51 (men) and 0·52 (women) (OR: 1·55, 95% CI: 1·01−2·38, $P = 0.047$), but not significant by waist-hip ratio (WHR) ≥ 0·85 (men) and 0·80 (women)[31] (OR: 1·27, 95% CI: 0·87−1·85, $P = 0.214$), after adjusting for potential confounders (Supplementary Table 3). This case-control study suggests that secreted GREM2 protein can be detected in human serum, and serum GREM2 levels are positively associated with general and central obesity.

Large-scale population study validates the positive association between serum GREM2 and central obesity
In the validation stage, we further measured serum GREM2 levels in a large-scale population including 10,327 participants.[22,23] General characteristics according to the quartiles of serum GREM2 levels are summarized in Supplementary Table 4. The prevalence of general obesity (defined by BMI) and central obesity (defined by WC, WHtR, or WHR) gradually increased as GREM2 levels increased ($P < 0.0001$ for all trends, Supplementary Table 4). Furthermore, serum GREM2 levels were positively correlated with BMI and WC in

the total population (Figure 1c,d). With the lowest quartile of serum GREM2 levels as the reference group, univariate logistic regression analysis showed significantly increased risks for general obesity, higher WC, higher WHtR, and higher WHR (Table 2). The association remained significant after adjustment for age and sex or after further adjustment for other potentially confounding factors (Table 2).

Furthermore, using GREM2 level as a continuous variable, the following significant ORs associated with a 1-SD increase of lnGREM2 levels were observed: 1·08 (95% CI, 1·04−1·13) for higher WC, 1·07 (95% CI, 1·03−1·11) for higher WHtR, and 1·05 (95% CI, 1·01−1·09) for higher WHR, after full adjustment for the covariates. A non-significant OR of 1·05 (95% CI, 1·00−1·10) for general obesity (BMI) was associated with a 1-SD increase of lnGREM2 levels (Supplementary Table 5). We then stratified the population and found the strongest association between lnGREM2 levels and WC in subjects with BMI $\leq$ 24·0 kg/m² (OR, 1·27; 95% CI, 1·04−1·54), compared with subjects with BMI $\geq$ 24·0 kg/m² (OR, 1·05; 95% CI, 1·00−1·11) (P for interaction < 0·0001, Supplementary Fig. 4). Next, we stratified all participants based on BMI and WC cutoffs. In each BMI category (BMI≤24·0, 24·0−28·0 or ≥28·0 kg/m²), according to the overweight/obesity criteria for China,[32] subjects with higher WC had higher GREM2 levels; whereas, in the subgroup with central obesity, serum GREM2 levels showed a decreasing trend in three BMI categories (Figure 1e). In this context, subjects with normal BMI (≤24·0 kg/m²) but central obesity (WC $\geq$ 90 cm [men] or ≥85 cm [women]) had the highest GREM2 levels in all six subgroups (Figure 1e). Together, these data indicate that serum GREM2 levels are more tightly associated with central obesity and relatively weakly associated with general obesity.

Elevated serum GREM2 levels and visceral fat deposits in humans

Excess fat accumulation in the abdominal cavity is a core feature of central obesity.[33,34] To evaluate the potential linkage between visceral fat content and serum GREM2 levels, the third independent cohort with 192 lean controls (mean BMI $\pm$ SD, 21·48 $\pm$ 1·81 kg/m²), 134 overweight (25·87 $\pm$ 1·15 kg/m²) and 250 obese individuals (32·08 $\pm$ 2·66 kg/m²) (Supplementary Table 6) received an abdominal-pelvic CT scan.[24] We calculated the visceral fat areas (VFAs) at the umbilical level (Figure 1f) using FatScan software[21,26] and whole visceral fat volume (VFV) using precise 3D CT reconstruction (Figure 1g) and defined a new obesity index, visceral fat content (VFC = VFV/body weight).[24] Of importance, we further confirmed the positive association between serum GREM2 levels and VFA, VFV, and VFC, respectively (Figure 1h−j). This cohort study

suggests that serum GREM2 levels are significantly associated with visceral fat deposits.

More Grem2 is secreted by visceral fat in adiposity status and its local expression is repressed during the browning process

Among various tissues of 8-week-old male C57BL/6J mice, eWAT (referred as classical visceral fat in mice) showed an abundant Grem2 mRNA expression (Figure 2a). After surgical removal of all eWAT pads, we detected a modest decrease in plasma Grem2 compared with sham-treated mice, suggesting a contribution of visceral fat to circulating Grem2 (Figure 2b). Physiologically, short-term fasting mobilizes visceral WAT more profoundly than subcutaneous WAT.[35] A marginal decrease of plasma Grem2 after 24 h fasting followed by a pronounced rebound after 24 h refeeding (Figure 2c). Furthermore, in *ob/ob* mice, Grem2 was elevated in the circulating system and eWAT (Figure 2d,e). Of importance, when the visceral fat pads isolated from *ob/ob* and WT mice were incubated *ex vivo*, *ob/ob* visceral fat secreted more Grem2 into extracellular fluids (Figure 2f,g). Interestingly, plasma Grem2 levels slightly declined following browning stimulation by short- and long-term cold stress in mice (Figure 2h). In consistence, under cold stress, a moderate reduction of Grem2 protein levels was detected in eWAT but not in inguinal white adipose tissue (iWAT) or BAT (Figure 2i). We thus isolated eWAT-derived SVFs and mature white adipocytes (MAs) from NCD and high-fat diet (HFD) mice, respectively, and found that Grem2 mRNA was preferentially expressed in MAs relative to SVFs (Figure 2j). Once primary SVFs were induced into mature beige adipocytes, a reduction in Grem2 mRNA expression and secreted Grem2 proteins were observed (Figure 2k,l). Together, these physiological and interventional results suggest that visceral fat releases more Grem2 in obese status, the circulating Grem2 levels fluctuate with visceral mass changes, and Grem2 might be involved in the browning process of visceral WAT.

Grem2 attenuates the browning capacity of visceral fat

A relatively weak browning capacity of visceral preadipocytes has been well described, when compared with subcutaneous preadipocytes.[3,8] We then pre-treated eWAT-derived SVFs of recombinant Grem2 protein only for 3 days before beige-adipocyte induction (Figure 3a). Despite with a low basal level, the mRNA and protein expression of uncoupled protein 1 (Ucp1), a brown/beige adipocyte marker, were detectable and could be inhibited by Grem2 in a concentration-dependent manner in differentiated mature beige adipocytes (Figure 3b,c). The expression of other BAT-related genes, including *Dio2* and *C/ebpβ*, was also reduced by
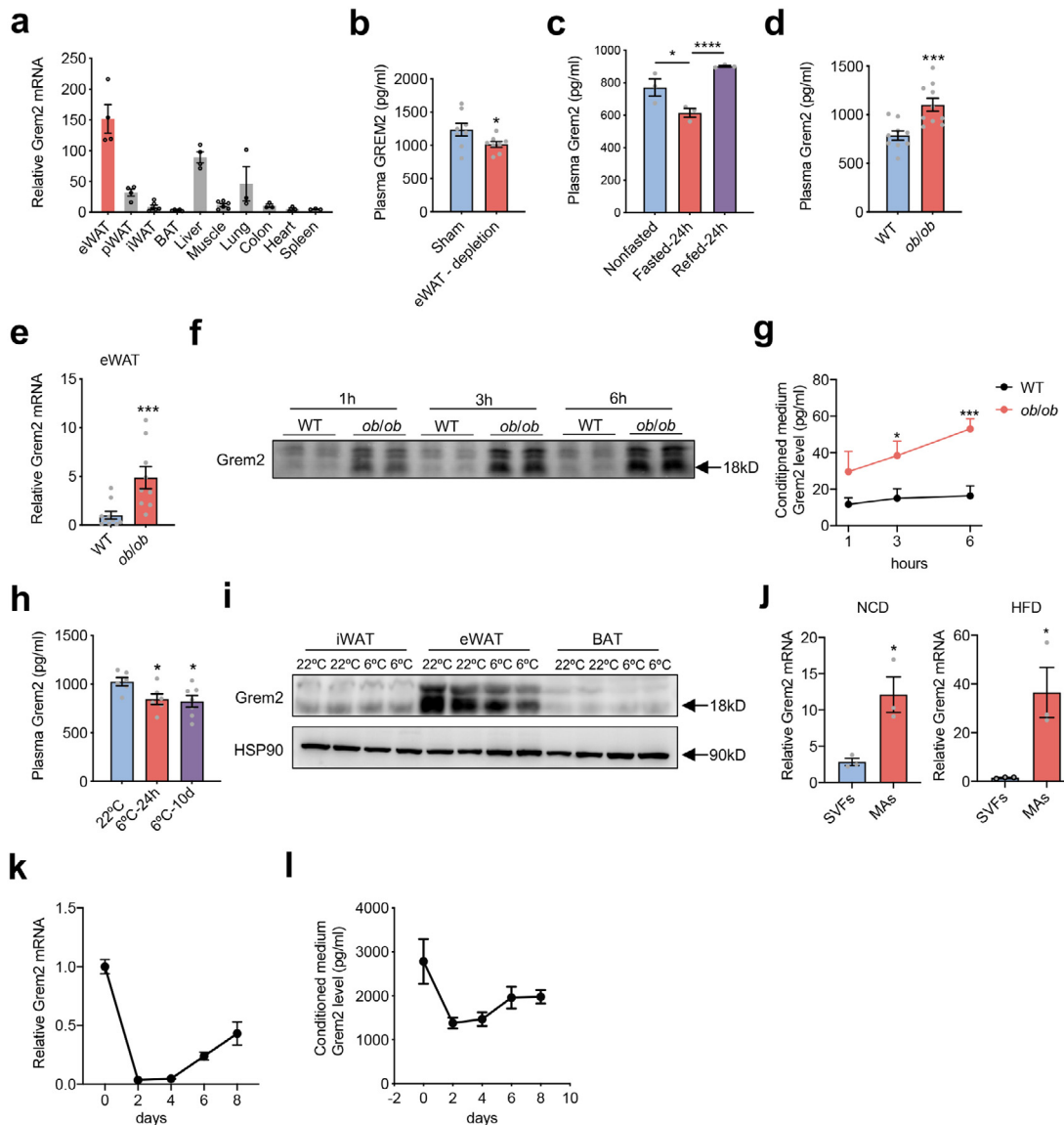
Figure 2. Plasma Grem2 levels change in response to various external stimuli. a. Relative mRNA levels of Grem2 in various tissues of mice ($n = 3−6$ per tissue). b. Plasma Grem2 levels in mice with surgical removal of bilateral eWATs ($n = 8$). c. 24 h fasting challenge induces plasma Grem2 reduction and refeeding promotes plasma Grem2 rebound in mice ($n = 3$). d. Plasma Grem2 levels in *ob/ob* mice ($n = 9−10$). e. Relative mRNA levels of Grem2 in eWAT of *ob/ob* mice ($n = 9−10$). f-g. The isolated visceral fat was incubated in conditioned media for 6 h that were sampled at 1 h, 3 h and 6 h, respectively. The Grem2 protein was detected by western blotting (f) and ELISA (g) methods ($n = 7$ for *ob/ob* and WT mice). h. Plasma Grem2 levels after short-term (24 h) and long-term (10 days) cold exposure ($n = 6$ for controls, 6 for short-term and 7 for long-term, respectively). i. Grem2 protein expression in eWAT, iWAT and BAT after 10-day cold exposure. j. Relative mRNA expression of Grem2 in SVFs and mature adipocytes (MAs) derived from eWAT from NCD-fed mice (left) and from HFD-fed mice (right) ($n = 3$). k. Relative mRNA expression of Grem2 after beige adipocyte induction of eWAT-derived SVFs ($n = 4$). l. Grem2 protein levels in conditioned medium after beige adipocyte induction of eWAT-derived SVFs ($n = 3$). For c and h, one-way ANOVA was used for the multiple group comparisons. For b, d, e, g and j, two-tailed Student's *t*-test was used for two group comparisons. Data are shown as mean ± SEM. * $p < 0.05$; ** $p < 0.01$; *** $p < 0.005$; **** $p < 0.001$.

high-concentration Grem2 treatment (Figure 3b). However, when the SVFs were induced with white-adipocyte induction cocktails (Figure 3d), the expression of white adipocyte markers was not significantly influenced by Grem2 (Figure 3e). In further, Grem2 inhibited the basal, uncoupled, and maximal oxygen consumption rates (OCRs) of induced beige adipocytes (Figure 3f). In consistence, Grem2 treatment also inhibited Ucp1 mRNA expression in the differentiated beige adipocytes derived from human visceral fat SVFs (Figure 3g).
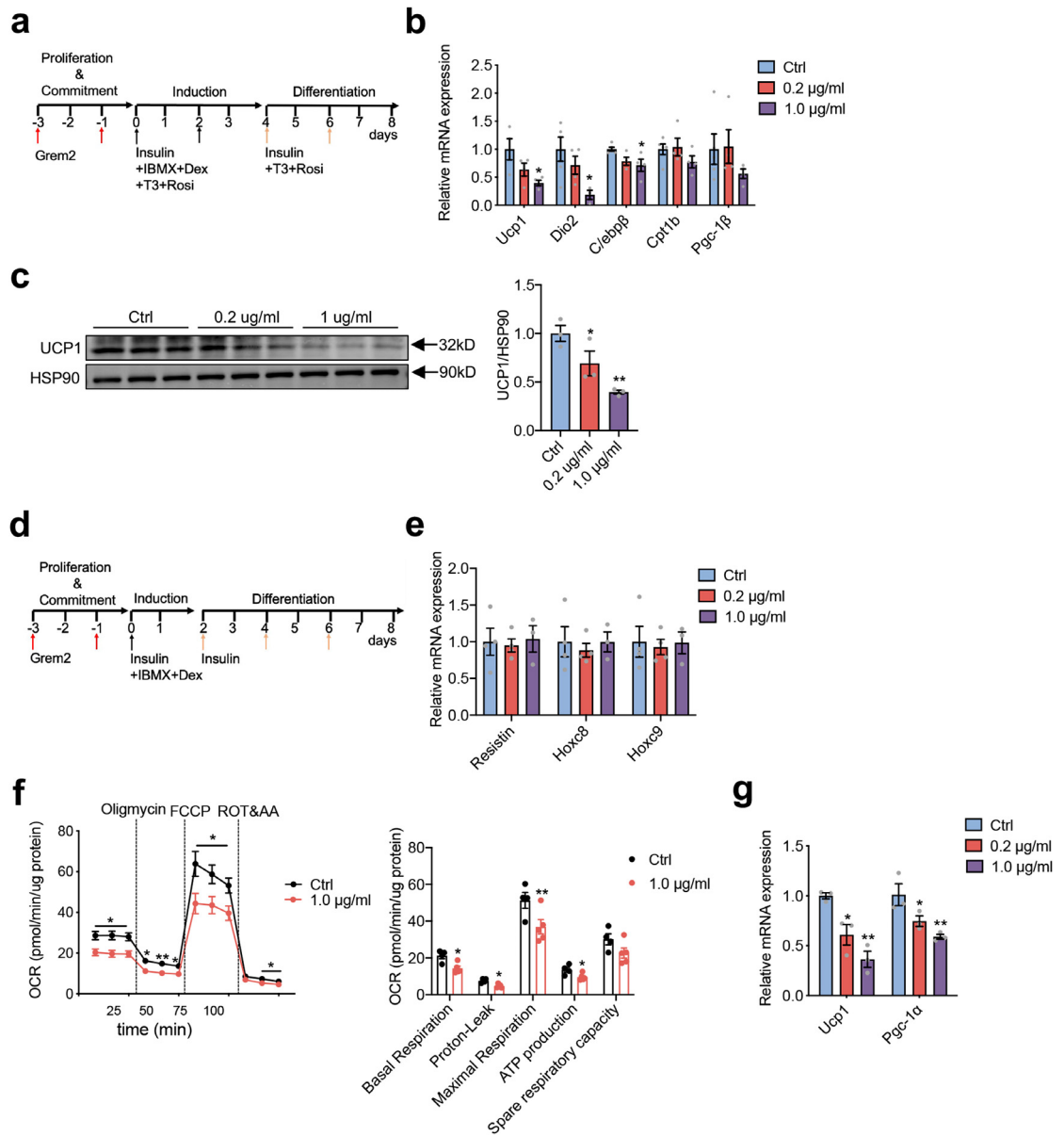
Figure 3. Grem2 inhibits the browning capacity of eWAT-derived preadipocytes *in vitro*. a. Differentiation protocol used for beige adipocytes derived from eWAT SVFs. b-c. Relative mRNA expression of thermogenic genes (*n* = 5 for control, 4 for 0·2 ug/ml, 1 ug/ml) (b), and Ucp1 protein levels and its quantification (c) in induced beige adipocytes of eWAT-derived SVFs with Grem2 pre-treatment for 3 days. d. Differentiation protocol used for white adipocytes derived from eWAT SVFs. e. Relative mRNA levels of white adipocytes-related genes in induced white adipocytes of eWAT-derived SVFs with Grem2 pre-treatment for 3 days (*n* = 4 for control, 0.2 ug/ml, 3 for 1 ug/ml). f. Oxygen consumption rates (OCRs) measurement of induced beige adipocytes (*n* = 4−5). g. Relative mRNA level of Ucp1 and Pgc-1α in induced beige adipocytes of human visceral WAT-derived SVFs with Grem2 pre-treatment (*n* = 3). For b, c, e, g, one-way ANOVA was used for the multiple group comparisons. For f, two-tailed Student's *t*-test was used for two group comparisons. PBS was used as control (Ctrl). Data are shown as mean $\pm$ SEM. *$p < 0.05$; **$p < 0.01$.

These results suggest that Grem2 may show a moderately inhibitory effect on the browning ability of visceral fat-derived preadipocytes *in vitro*.

Further supporting evidence was collected in *Grem2* transgenic (*Grem2*[Tg]) mice (Supplementary Fig. 5a). Grem2 was overexpressed in eWAT (Figure 4a,b) and other tissues (Supplementary Fig. 5b−d). Compared with WT mice, *Grem2*[Tg] mice showed no significant changes in glucose tolerance or food intake (Supplementary Fig. 5e,f). Despite the detection of unchanged energy expenditure, including O$_2$ consumption, CO$_2$ production, or physical activity under normal condition
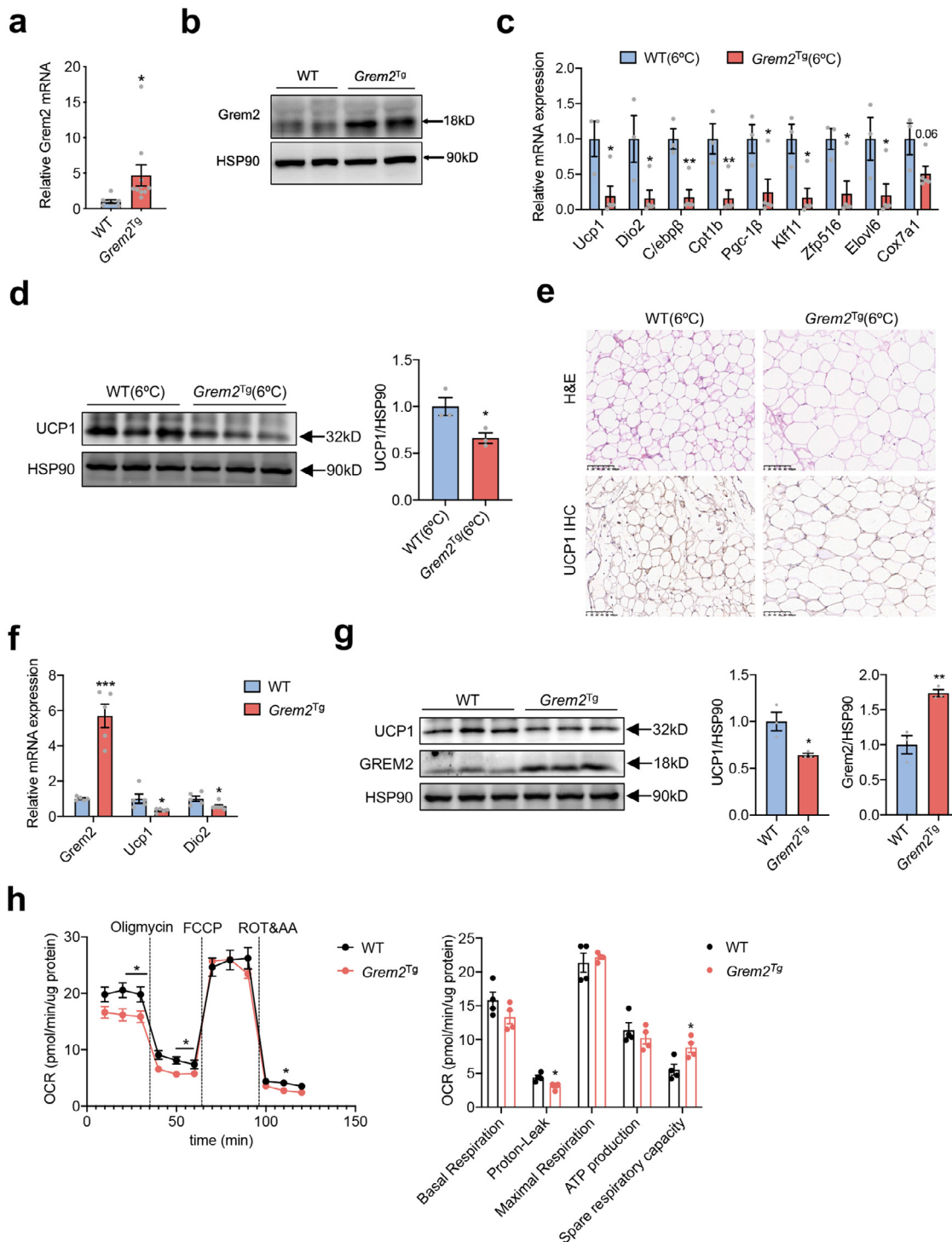
Figure 4. Attenuated browning abilities of visceral fat in *Grem2* transgenic (termed *Grem2*^Tg) mice. a-b. Relative mRNA (a) and protein (b) levels of Grem2 in eWAT of *Grem2*^Tg and WT mice, respectively ($n = 8-10$). c. Relative mRNA levels of thermogenic genes in the eWAT of both groups under cold exposure for 10 days ($n = 3-5$). d. Representative western blotting (left) and the quantification (right) of Ucp1 levels in eWAT of both groups for 10-day coldness. HSP90 were used as internal controls. e. Representative H&E and immunohistochemical (IHC) staining of Ucp1 in the eWAT treated as (d). Scale bar, 100 μm. f-h. Relative mRNA levels of Grem2 and thermogenic genes ($n = 5$) (f), the protein levels of Grem2 and Ucp1 (left), and their quantification (right) (g), and OCRs measurement ($n = 4$) (h) in fully differentiated eWAT-derived beige adipocytes of both groups *ex vivo*. For a, c, d, f-h, two-tailed Student's *t*-test was used for two group comparisons. Data are shown as mean $\pm$ SEM. * $p < 0.05$; ** $p < 0.01$; *** $p < 0.005$.

(Supplementary Fig. 5g−i), the expression of browning-related genes was repressed in eWAT of $Grem2^{Tg}$ mice after 10 days of cold stimulation (6 °C) (Figure 4c). No significant change of adipogenesis and chronic inflammation genes was detected (Supplementary Fig. 5j,k). Under cold stress, Ucp1 protein expression was mildly attenuated by Grem2 overexpression (Figure 4d), and $Grem2^{Tg}$ mice exhibited weaker Ucp1 staining and larger adipocytes compared with those of WT mice (Figure 4e). By inducing eWAT-derived SVFs of $Grem2^{Tg}$ and WT mice into mature beige adipocytes, we also observed a moderately repressed Ucp1 expression (Figure 4f,g) and decreased uncoupled OCR levels (Figure 4h) in Grem2-overexpressed beige adipocytes.

Grem2 ablation mildly enhances the browning capacity of visceral fat

We further generated adipose Grem2 knockout mice by crossing $Grem2^{flox/flox}$ mice with $aP2$-cre mice ($Grem2$-$^{flox/flox}$;$aP2$-cre, termed AGKO mice; Supplementary Fig. 6a), as $aP2$-cre was reported to delete target genes mainly in adipocytes and a proportion of preadipocytes.[36] As expected, AGKO mice showed Grem2 deficiency in eWAT (Figure 5a) and other adipose tissues (Supplementary Fig. 6b,c). In growth curves under NCD, AGKO mice displayed mildly decreased body weights (Figure 5b) as well as reduced visceral fat mass (Figure 5c and Supplementary Fig. 6d), while no significant change in blood glucose, food intake, and energy expenditure was observed under nomal condition (Supplementary Fig. 6e−i). No obvious change of adipogenesis and chronic inflammation genes was observed (Supplementary Fig. 6j,k). Of note, under cold stress, enhanced browning features such as increased Ucp1 mRNA and protein expression and smaller adipocytes with Ucp1 positive staining were observed in eWAT of AGKO mice (Figure 5d−f). These data indicate that ablation of Grem2 mildly promotes the browning capacity of visceral fat and is associated with reduced visceral fat content.

Grem2 binds to BMP4/7 and inhibits the browning capacity of visceral preadipocytes partially via the BMP4/7-BMPR2-SMADs signaling pathway

Consistent with previous findings that demonstrated the promotional roles of BMP4 and BMP7 in the browning progress of sWAT,[37,38] in this study, we found that both BMP4 and BMP7 also enhanced the browning capacity of eWAT-derived SVFs in a concentration-dependent manner *in vitro* (Supplementary Fig. 7a,b). Then, recombinant Grem2 protein was combined with BMP4 and BMP7 treatment, respectively, to treat preadipocytes for 3 days before induction. Interestingly, we found that Grem2 significantly attenuated the promotional effects of BMP4 and BMP7 on the expression of

Ucp1 and other browning-related genes (Figure 6a−d). Using Oil Red O staining, we also revealed that both BMP4 and BMP7 promoted lipid droplet formation in mature beige adipocytes, while the preadipocytes treated with Grem2 alone or in combination with BMP4/7 showed fewer lipid droplets than the corresponding control groups (Supplementary Fig. 7c,d). Next, we revealed that Grem2 could interact to both BMP4 and BMP7 proteins (Supplementary Fig. 7e,f). The binding of BMP dimers to their receptor complex activates the type II receptor (BMPRII in adipose tissue) to phosphorylate the type I receptor (BMPRI), which in turn activates the regulatory canonical SMAD pathway or p38 in the non-canonical pathway.[39,40] To evaluate the potential involvement of the BMP receptor complex of preadipocytes in the process of Grem2 antagonizing BMP4/7, we generated preadipocyte $Bmpr2$ knockout mice by crossing $Bmpr2^{f/f}$ mice[27] with $Pdgfr\alpha$-cre mice[36] ($Bmpr2^{f/f}$;$Pdgfr\alpha$-cre, termed pBRKO). Following the induction of beige adipocyte cocktails *ex vivo*, the browning capacity of visceral preadipocytes was largely attenuated in pBRKO mice compared with control mice (Figure 6e−h). Furthermore, Grem2 could not inhibit the mRNA and protein expression of Ucp1 in differentiated beige adipocytes derived from $Bmpr2$-deficient preadipocytes; and more importantly, the antagonizing effects of Grem2 on BMP4/7′s browning ability was largely attenuated under the $Bmpr2$-deficient condition. Finally, we found that both BMP4 and BMP7 enhanced the phosphorylation of SMAD1/5/8 in visceral preadipocytes, which could be repressed by additional Grem2 treatment; however, the p38MAPK signaling pathway was not inhibited by Grem2 treatment (Figure 6i,j). In addition, Grem2 could not antagonize BMP4/7′s effects on canonical Wnt signaling (Supplementary Fig. 8a,b) or the expression of Wnt downstream target genes (Supplementary Fig. 8c,d). Taken together, these results suggest that the inhibitory role of Grem2 in the browning process of visceral fat could be, in part at least, attributed to its inhibition of the BMP4/7-BMPR2-SMAD signaling pathway in visceral preadipocytes.

Discussion

In this study, we performed translational research to identify a circulating protein associated with visceral adiposity. Using an ELISA method, we measured circulating GREM2 levels in three independent cohorts, and reported that GREM2 was elevated in obese individuals and was more strongly associated with central obesity and visceral fat content than general obesity. Interestingly, visceral fat secreted more Grem2 into extracellular fluids in adiposity status, and circulating Grem2 levels were associated with the changes of visceral fat content and fluctuated in response to external calorie supplies. Moreover, using transgenic mouse models, we revealed that Grem2 overexpression reduced the
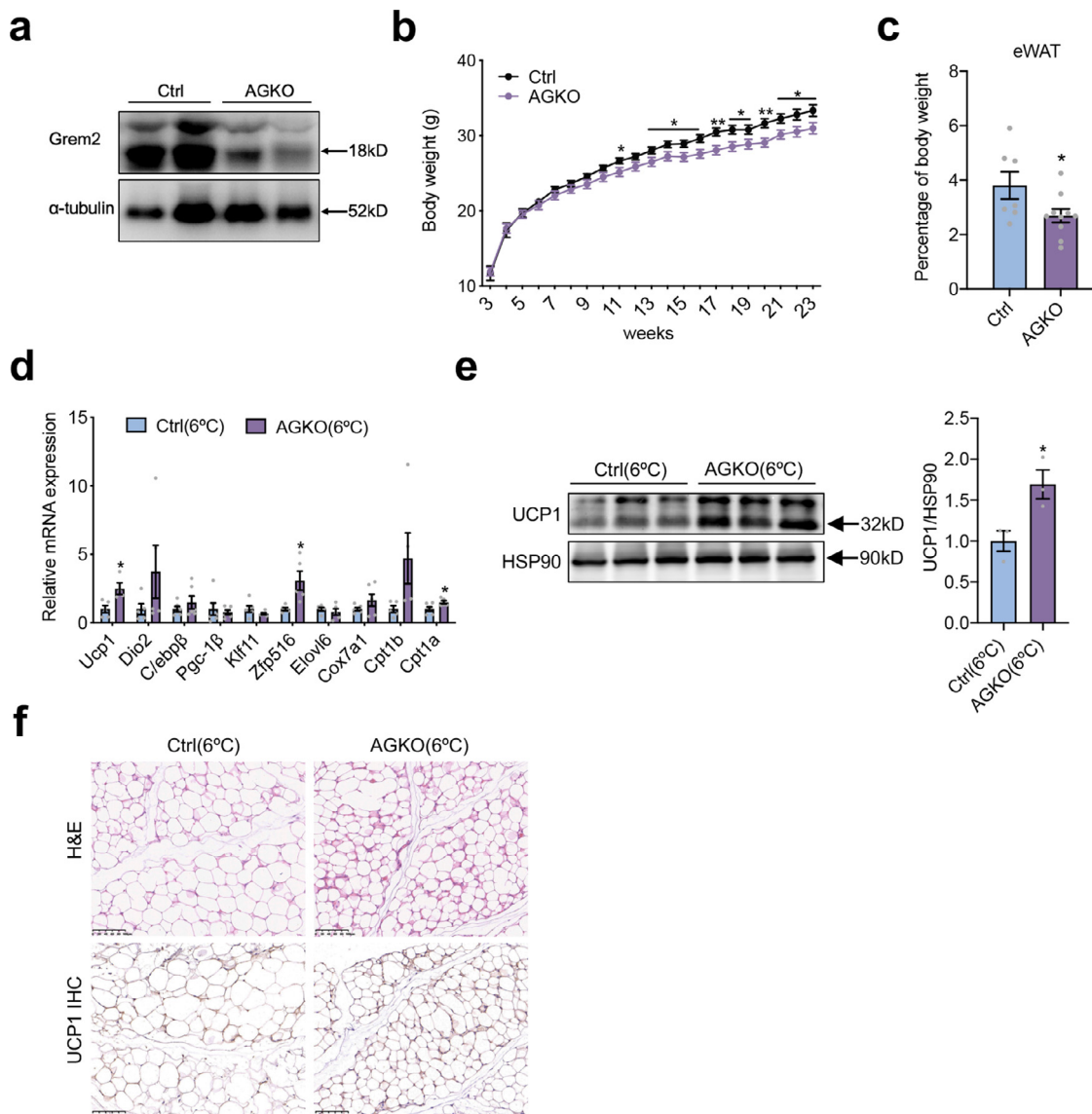
Figure 5. Enhanced browning abilities of visceral fat and reduced visceral fat content in *Grem2* knockout mice. a. The protein levels of Grem2 in eWAT of *Grem2*^floxp/floxp;*aP2*-cre (termed AGKO) and littermate control mice. b. Body weight curve of AGKO and control mice ($n = 12$). c. eWAT content of AGKO and control mice ($n = 7-10$). d-f. Relative mRNA levels of thermogenic genes ($n = 5-6$) (d), the protein levels of Ucp1 (left) and their quantification (right) (e), and representative H&E and IHC staining of Ucp1($n = 3$) (f) in the eWAT of both groups for 10-day coldness. Scale bar, 100 μm. For b-e, two-tailed Student's *t*-test was used for two group comparisons. Data are shown as mean $\pm$ SEM. * $p < 0.05$; **$p < 0.01$.

browning capacity of visceral fat, while Grem2 deficiency promoted the browning capacity of visceral fat and mildly reduced visceral fat content. In cellular and molecular experiments, Grem2 antagonizes the BMP4/7-BMPR2-SMAD signaling pathway in preadipocytes and attenuated their browning capacity.

The concept of central obesity was first proposed by Vague et al. in the 1940s.[41] Central obesity is considered a stronger independent risk factor for cardiometabolic disorders than general obesity.[3,4] The NHANES III cohort study disclosed that subjects with normal-weight central obesity had the worst long-term survival.[42] In contrast to the routine index of central obesity (such as WC and WHR), the exact quantification of visceral fat mass and content with whole-visceral cavity CT or Magnetic Resonance Imaging (MRI) scanning is scarce at present clinical practices, which also impedes the identification of visceral adiposity-related serum biomarkers. This study demonstrated the association between circulating GREM2 levels and visceral fat mass with a
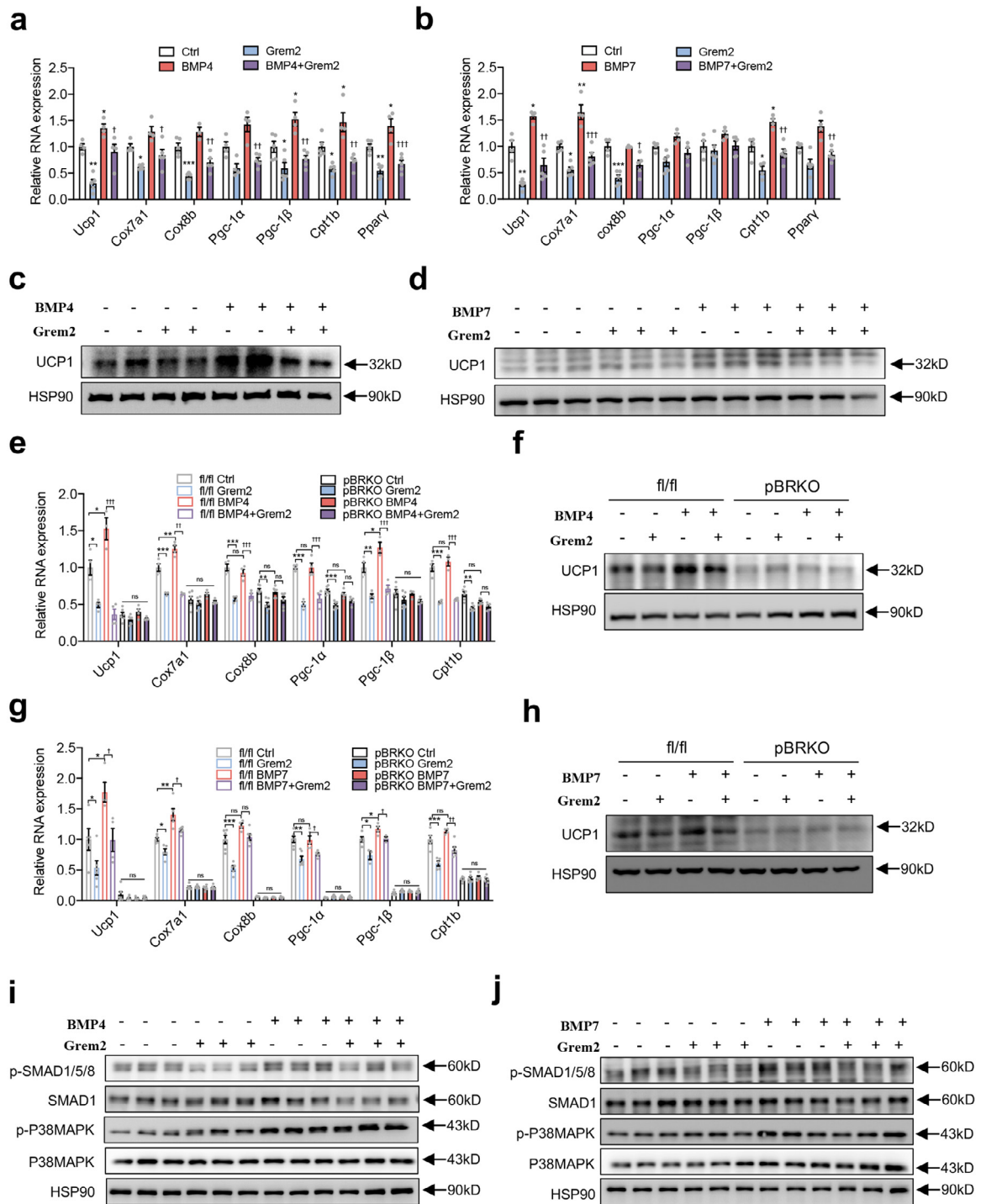
Figure 6. Grem2 inhibits the browning capacity of visceral preadipocytes partially via BMP4/7-BMPR2 signaling pathway. a-d. Relative mRNA levels of thermogenic genes ($n = 4-5$) (a and b) and the protein levels of Ucp1 (c and d) in induced beige adipocytes from visceral preadipocytes pre-treated with Grem2 in addition to BMP4 (a and c) or Bmp7 (b and d), respectively, for 3 days before induction. e-h. The mRNA expression of thermogenic genes ($n = 4-6$) (e and g) and the protein level of Ucp1 (f and h) in induced beige adipocytes from *Bmpr2*^floxp/floxp;*Pdgfrα*-cre (termed pBRKO) and *Bmpr2*^floxp/floxp-derived visceral preadipocytes pre-treated with Grem2 in addition to BMP4 (e and f) or BMP7 (g and h), respectively, for 3 days before induction. i-j. The protein levels of phosphorated and total SMAD1/5/8 and p38MAPK proteins in visceral preadipocytes treated with Grem2 in addition to BMP4 (i) and BMP7 (j), respectively, for one hour. For a-b, e and g, one-way ANOVA was used for the multiple group comparisons. Data are shown as mean ± SEM. *, †$p < 0.05$; **, ††$p < 0.01$; ***, †††$p < 0.001$.

deeply-phenotyped cohort.[24] More importantly, our large-scale general communication population found that normal-weight central obesity had the highest serum GREM2 concentrations among all subgroups (including those with high BMI).

In addition, with the GOCY cohort, we have successfully identified certain underlying genetic factors, such as the functional variants in *LGR4* and *NPC1*, associated with high visceral WAT content.[19,20] Unfortunately, we did not detect statistically significant genetic variations in the human *GREM2* gene (data not shown). However, to the best of our knowledge, there is no evidence regarding the relationship between serum GREM2 and human visceral obesity, particularly visceral fat mass. Last year, Hedjazifar et al. reported that GREM1, which is also highly expressed in visceral fat, was increased in obese subjects, especially those with type 2 diabetes, nonalcoholic fatty liver disease (NAFLD), and nonalcoholic steatohepatitis (NASH),[43] the role of GREM2 in these obesity-related metabolic disorders such as diabetes warrants further investigation. In future, the longitudinal cohorts, such as long-term follow-ups of weight-loss intervention or weight-gain population, are important to strengthen these cross-sectional observations.

Mouse Grem2 was highly expressed in eWAT (predominantly in mature adipocytes) and liver; surgically removing eWAT moderately decreased circulating Grem2 levels by approximately 20%. Given the difference in Grem2 concentrations between *in vitro* administration (μg/ml) and in circulating detection (ng/ml), it is thus hypothesized that the interstitial concentrations of Grem2 are probably higher than those in circulation, and Grem2 might inhibit the browning capacity of visceral preadipocytes mainly in a paracrine/autocrine way but not in an endocrine way. Obesity is characterized with low browning ability of WATs.[3,6] More Grem2 is secreted outside of visceral fat (mature adipocytes) and to some extent contribute to the total circulating Grem2 pool when visceral adiposity occurs. Of note, we could not exclude the possibility that the liver, another organ with high Grem2 expression, may compensate by secreting even more Grem2 into the circulation after eWAT removal or upon the development of visceral adiposity and NAFLD/NASH. However, other experimental data, especially for Grem2 concentrations in the portal vein and different fat depots, still require extensive evidence in human subjects under various pathophysiological stimuli.[15] In addition, the expression profile of GREM2 in various human tissues needs more detailed characterization.

Visceral white adipocytes are commonly regarded as inert and inconvertible to beige adipocytes.[3] Although the underlying factors remain poorly understood, BMPs have been identified as distinct factors in the browning capacity of different fat depots.[8] Consistently, we showed that BMP4/7 addition before induction could also promote the differentiation and browning capacity

of visceral preadipocytes. Notably, Grem2 could bind to BMP4/7 and attenuated the promoting effects of BMP4/7 on cell fate determination to browning adipocyte differentiation.[44] Other studies have demonstrated that downstream SMAD1/5/8 signaling has a role in lineage determination, whereas p38/MAPK signaling only shows minor effects on commitment efficiency.[45] It was assumed that the various local-concentration ratios of BMP antagonists (such as GREM1/2) to BMPs (like BMP4/7) might contribute to biased activation of downstream pathway and further the intrinsic browning capacity of preadipocytes in different fat depots, which also needs further investigations.

A mature BMPs-BMPR signaling complex requires one ligand dimer firstly to bind two type II receptors and then recruit two type I receptors.[40] Brown fat paucity due to ablation of Bmpr1a induces a robust compensatory browning change in white fat,[46] whereas the ablation of Bmpr2 in preadipocytes (Pdgfrα^+) has not yet been reported. This study found that pBRKO mice showed a similar growth and body weight phenotype to our previously reported adipose tissue *Bmpr2* knockout mice[47] but had an earlier defect in WAT development. The preadipocytes derived from visceral fat depots of pBRKO mice exhibited a weaker differentiation capacity of beige adipocytes than those of control mice. In the *Bmpr2*-deficient context, the antagonistic effects of Grem2 on BMP4/7 in the adipogenesis of beige adipocytes were largely attenuated, suggesting an important role of GREM2-BMP4/7-BMPR2-SMAD signaling in the modulation of the inert browning capacity of visceral fat. However, whether other BMPs and BMP receptors are also involved in the process remains unclear, and the way Grem2-BMP4/7-BMPR2 signaling axis specifically functions on the visceral fat but not on other fat depots also warrants further investigation.

It should be noted that we did not detect any significant energy expenditure changes either in *Grem2*-transgenic or *Grem2* knockout mice. One possible explanation is that the contribution of visceral fat browning in whole-body energy expenditure might be too subtle to be detected in mice by the presently available instruments, as we indeed revealed changes in mitochondrial respiration in *Grem2*-transgenic beige adipocytes *ex vivo*. Given that a one-unit increase in visceral fat mass was associated with a 7·3-fold higher risk of type 2 diabetes,[48] selectively targeting visceral fat in clinical practice is promising and would more effectively reduce the complications related to visceral adiposity.[49,50] In combating visceral obesity, a probability remains that improving the browning ability of visceral fat, such as by functional blockade of GREM2, may lead to long-term metabolic benefits. Of note, several physiological and biological questions regarding the roles of blood Grem2 on metabolic traits remain to be answered. For instance, which tissues are the main source and target of blood Grem2, and whether Grem2

could function in an endocrine way to regulate fat mass. Finding answers to these important questions will provide new insights not only into visceral adiposity but also into the whole-body signaling network that maintains metabolic homeostasis during obesity.

Conclusion

This study reports that GREM2 appears to be a circulating protein factor as an independent variable correlated to visceral obesity. In addition, we suggest a potential molecular mechanism underlying Grem2 inhibiting the browning capacity of visceral preadipocytes. These findings highlight the possibility of targeting GREM2 and its downstream pathways for obesity stratification and clinical intervention of human visceral adiposity.

Contributors

Conceptualization, J.Q.W.; Methodology, J.Q.W., W.Liu, D.L., and L.W.; Experiment, W.Liu, D.L., M.L.Y., R.X.L., L.W., Y.X., and Z.Y.Z.; Material, S.W.Q, and Q.Q.T.; Investigation, W.Li, S.Q.Z., A.B.G., N.C., Q.Y.M., R.Z. Z, and S.J.W.; Writing − Original Draft, W.Liu and L. W.; Writing − Review & Editing, J.Q.W. and R.X.L.; Funding Acquisition, J.Q.W., G.N., W.Q.W., R.X.L. Y. Hong.C., and W.Liu; Human Resources, J.Q.W., G.N., W.Q.W., Y.X., J.H., W.Q.G, Y.F.Z, J.S., Y.Fei.C., Y. Hong.C., and Y.F.B., W.Liu, D.L., M.L.Y., L.W. and Y.X. verified the underlying data. D.L. and R.X.L. provided critical feedback in the revision of the manuscript. All authors read and approved the final manuscript.

Data sharing statement

The expression profile of visceral WAT in *Lgr4*-deficient mice has been deposited in GEO (GSE195570). Summary data are available in the paper and in supplementary materials. Raw data that support the findings of this study are available from the corresponding author upon request.

Declaration of interests

The authors have declared that no conflict of interest exists.

Acknowledgements

Supplementary materials

Supplementary material associated with this article can be found in the online version at doi:10.1016/j.ebiom.2022.103969.

References

1 Collaboration NCDRF. Trends in adult body-mass index in 200 countries from 1975 to 2014: a pooled analysis of 1698 population-based measurement studies with 19.2 million participants. *Lancet.* 2016;387(10026):1377–1396.

2 Cypess AM. Reassessing Human Adipose Tissue. *N Engl J Med.* 2022;386(8):768–779.

3 Giordano A, Frontini A, Cinti S. Convertible visceral fat as a therapeutic target to curb obesity. *Nat Rev Drug Discov.* 2016;15(6):405–424.

4 Coutinho T, Goel K, Correa de Sa D, et al. Combining body mass index with measures of central obesity in the assessment of mortality in subjects with coronary disease: role of "normal weight central obesity". *J Am Coll Cardiol.* 2013;61(5):553–560.

5 Ngo DTM, Sverdlov AL, Karki S, et al. Oxidative modifications of mitochondrial complex II are associated with insulin resistance of visceral fat in obesity. *Am J Physiol Endocrinol Metab.* 2019;316(2): E168–EE77.

6 Cohen P, Kajimura S. The cellular and functional complexity of thermogenic fat. *Nat Rev Mol Cell Biol.* 2021;22(6):393–409.

7 Harms M, Seale P. Brown and beige fat: development, function and therapeutic potential. *Nat Med.* 2013;19(10):1252–1263.

8 Macotela Y, Emanuelli B, Mori MA, et al. Intrinsic differences in adipocyte precursor cells from different white fat depots. *Diabetes.* 2012;61(7):1691–1699.

9 Fukuhara A, Matsuda M, Nishizawa M, et al. Visfatin: a protein secreted by visceral fat that mimics the effects of insulin. *Science.* 2005;307(5708):426–430.

10 Berndt J, Kloting N, Kralisch S, et al. Plasma visfatin concentrations and fat depot-specific mRNA expression in humans. *Diabetes.* 2005;54(10):2911–2916.

11 Moerman EJ, Teng K, Lipschitz DA, Lecka-Czernik B. Aging activates adipogenic and suppresses osteogenic programs in mesenchymal marrow stroma/stem cells: the role of PPAR-gamma2 transcription factor and TGF-beta/BMP signaling pathways. *Aging Cell.* 2004;3(6):379–389.

12 Qian SW, Tang Y, Li X, et al. BMP4-mediated brown fat-like changes in white adipose tissue alter glucose and energy homeostasis. *Proc Natl Acad Sci U S A.* 2013;110(9):E798–E807.

13 Qian S, Tang Y, Tang QQ. Adipose tissue plasticity and the pleiotropic roles of BMP signaling. *J Biol Chem.* 2021;296: 100678.

14 Tseng YH, Kokkotou E, Schulz TJ, et al. New role of bone morphogenetic protein 7 in brown adipogenesis and energy expenditure. *Nature.* 2008;454(7207):1000–1004.

15 Kawagishi-Hotta M, Hasegawa S, Igarashi T, et al. Increase of gremlin 2 with age in human adipose-derived stromal/stem cells and its inhibitory effect on adipogenesis. *Regen Ther.* 2019;11:324–330.

16 Wu Q, Tang SG, Yuan ZM. Gremlin 2 inhibits adipocyte differentiation through activation of Wnt/beta-catenin signaling. *Mol Med Rep.* 2015;12(4):5891–5896.

17 Wang CL, Xiao F, Wang CD, et al. Gremlin2 suppression increases the BMP-2-induced osteogenesis of human bone marrow-derived mesenchymal stem cells via the BMP-2/Smad/Runx2 signaling pathway. *J Cell Biochem.* 2017;118(2):286–297.

18 Yanagita M. BMP antagonists: their roles in development and involvement in pathophysiology. *Cytokine Growth Factor Rev.* 2005;16(3):309–317.

19 Wang J, Liu R, Wang F, et al. Ablation of LGR4 promotes energy expenditure by driving white-to-brown fat switch. *Nat Cell Biol.* 2013;15(12):1455–1463.

20 Liu R, Zou Y, Hong J, et al. Rare loss-of-function variants in NPC1 predispose to human obesity. *Diabetes.* 2017;66(4):935–947.

21 Liu R, Hong J, Xu X, et al. Gut microbiome and serum metabolome alterations in obesity and after weight-loss intervention. *Nat Med.* 2017;23(7):859–868.

22 Ding L, Song A, Dai M, et al. Serum lipoprotein (a) concentrations are inversely associated with T2D, prediabetes, and insulin resistance in a middle-aged and elderly Chinese population. *J Lipid Res.* 2015;56(4):920–926.

23 Li M, Xu Y, Xu M, et al. Association between nonalcoholic fatty liver disease (NAFLD) and osteoporotic fracture in middle-aged and elderly Chinese. *J Clin Endocrinol Metab.* 2012;97(6):2033–2038.

24 Shi J, Bao G, Hong J, et al. Deciphering CT texture features of human visceral fat to evaluate metabolic disorders and surgery-induced weight loss effects. *EBioMedicine.* 2021;69: 103471.

25 Ye L, Gu W, Chen Y, et al. The impact of shift work on glycemic characteristics assessed by CGM and its association with metabolic indices in non-diabetic subjects. *Acta Diabetol.* 2020;57(1):53–61.

26 Zou Y, Ning T, Shi J, et al. Association of a gain-of-function variant in LGR4 with central obesity. *Obesity.* 2017;25(1):252–260. (Silver Spring).

27 Qian SW, Wu MY, Wang YN, et al. BMP4 facilitates beige fat biogenesis via regulating adipose tissue macrophages. *J Mol Cell Biol.* 2019;11(1):14–25.

28 Chen M, Lu P, Ma Q, et al. CTNNB1/beta-catenin dysfunction contributes to adiposity by regulating the cross-talk of mature adipocytes and preadipocytes. *Sci Adv.* 2020;6(2):eaax9605.

29 Parikh RM, Joshi SR, Pandia K. Index of central obesity is better than waist circumference in defining metabolic syndrome. *Metab Syndr Relat Disord.* 2009;7(6):525–528.

30 Amato MC, Giordano C, Galia M, et al. Visceral adiposity index: a reliable indicator of visceral fat function associated with cardiometabolic risk. *Diabetes Care.* 2010;33(4):920–922.

31 Jensen MD, Ryan DH, Apovian CM, et al. 2013 AHA/ACC/TOS guideline for the management of overweight and obesity in adults: a report of the American college of cardiology/American heart association task force on practice guidelines and the obesity society. *J Am Coll Cardiol.* 2014;63(25 Pt B):2985–3023.

32 Pan XF, Wang L, Pan A. Epidemiology and determinants of obesity in China. *Lancet Diabetes Endocrinol.* 2021;9(6):373–392.

33 Karlsson T, Rask-Andersen M, Pan G, et al. Contribution of genetics to visceral adiposity and its relation to cardiovascular and metabolic disease. *Nat Med.* 2019;25(9):1390–1395.

34 Lotta LA, Wittemans LB, Zuber V, et al. Association of genetic variants related to gluteofemoral vs abdominal fat distribution with type 2 diabetes, coronary disease, and cardiovascular risk factors. *JAMA.* 2018;320(24):2553–2563.

35 Ding H, Zheng S, Garcia-Ruiz D, et al. Fasting induces a subcutaneous-to-visceral fat switch mediated by microRNA-149-3p and suppression of PRDM16. *Nat Commun.* 2016;7:11533.

36 Krueger KC, Costa MJ, Du H, Feldman BJ. Characterization of Cre recombinase activity for *in vivo* targeting of adipocyte precursor cells. *Stem Cell Rep.* 2014;3(6):1147–1158.

37 Schulz TJ, Huang TL, Tran TT, et al. Identification of inducible brown adipocyte progenitors residing in skeletal muscle and white fat. *Proc Natl Acad Sci U S A.* 2011;108(1):143–148.

38 Hoffmann JM, Grunberg JR, Church C, et al. BMP4 gene therapy in mature mice reduces BAT activation but protects from obesity by browning subcutaneous adipose tissue. *Cell Rep.* 2017;20(5):1038–1049.

39 Blazquez-Medela AM, Jumabay M, Bostrom KI. Beyond the bone: Bone morphogenetic protein signaling in adipose tissue. *Obes Rev.* 2019;20(5):648–658.

40 Schmierer B, Hill CS. TGFbeta-SMAD signal transduction: molecular specificity and functional flexibility. *Nat Rev Mol Cell Biol.* 2007;8(12):970–982.

41 Vague J. A determinant factor of the forms of obesity. *Obes Res.* 1996;4(2):201–203.

42 Sahakyan KR, Somers VK, Rodriguez-Escudero JP, et al. Normal-weight central obesity: implications for total and cardiovascular mortality. *Ann Intern Med.* 2015;163(11):827–835.

43 Hedjazifar S, Khatib Shahidi R, Hammarstedt A, et al. The Novel adipokine gremlin 1 antagonizes insulin action and is increased in type 2 diabetes and NAFLD/NASH. *Diabetes.* 2020;69(3):331–341.

44 Elsen M, Raschke S, Tennagels N, et al. BMP4 and BMP7 induce the white-to-brown transition of primary human adipose stem cells. *Am J Physiol Cell Physiol.* 2014;306(5):C431–C440.

45 Huang H, Song TJ, Li X, et al. BMP signaling pathway is required for commitment of C3H10T1/2 pluripotent stem cells to the adipocyte lineage. *Proc Natl Acad Sci U S A.* 2009;106(31):12670–12675.

46 Schulz TJ, Huang P, Huang TL, et al. Brown-fat paucity due to impaired BMP signalling induces compensatory browning of white fat. *Nature.* 2013;495(7441):379–383.

47 Qian S, Pan J, Su Y, et al. BMPR2 promotes fatty acid oxidation and protects white adipocytes from cell death in mice. *Commun Biol.* 2020;3(1):200.

48 Karlsson T, Rask-Andersen M, Pan G, et al. Contribution of genetics to visceral adiposity and its relation to cardiovascular and metabolic disease. *Nat Med.* 2019;25(9):1390–1395.

49 Rodriguez A, Catalan V, Gomez-Ambrosi J, Fruhbeck G. Visceral and subcutaneous adiposity: are both potential therapeutic targets for tackling the metabolic syndrome? *Curr Pharm Des.* 2007;13(21):2169–2175.

50 Smith SR, Zachwieja JJ. Visceral adipose tissue: a critical review of intervention strategies. *Int J Obes Relat Metab Disord.* 1999;23(4):329–335.